

Structures, Symmetries, Mechanics and Motors of carbon nanotubes

Z. C. Tu and Z. C. Ou-Yang

*Institute of Theoretical Physics, The Chinese Academy of Sciences
P.O.Box 2735 Beijing 100080, China*

ABSTRACT

The structures and symmetries of single-walled carbon nanotubes (SWNTs) are introduced in detail. The physical properties of SWNTs induced by their symmetries can be described by tensors in mathematical point of view. It is found that there are 2, 4, and 5 different parameters in the second, third, and fourth rank tensors representing electronic conductivity (or static polarizability), the second order nonlinear polarizability, and elastic constants of SWNTs, respectively. The values of elastic constants obtained from tight-binding method imply that SWNTs might be very weakly anisotropic in mechanical properties. The further study on the mechanical properties shows that the elastic shell theory in the macroscopic scale can be applied to carbon nanotubes (CNTs) in the mesoscopic scale, as a result, SWNTs can be regarded as an isotropic material with Poisson ratio, effective thickness, and Young's modulus being $\nu = 0.34$, $h = 0.75\text{\AA}$, $Y = 4.70\text{TPa}$, respectively, while the Young's moduli of multi-walled carbon nanotubes (MWNTs) are apparent functions of the number of layers, N , varying from 4.70TPa to 1.04TPa for $N = 1$ to ∞ . Based on the chirality of CNTs, it is predicted that a new kind of molecular motor driven by alternating voltage can be constructed from double walled carbon nanotubes (DWNTs).

INTRODUCTION

Carbon is the core element to construction of organic matters and has always attracted much attention up to now. Many decades ago, people only knew two kinds of crystals consisting of carbon: graphite with layer structure and diamond with tetrahedral shape. The situation was changed in 1985 when Kroto *et al.* synthesized bucky ball—a football-like molecule consisting of 60 carbon atoms [1] which marked the beginning of carbon times. After that, Iijima synthesized MWNTs in 1991 [2] and SWNTs in 1993 [3]. Simply speaking, a SWNT can be regarded as a graphitic sheet with hexagonal lattices that was wrapped up into a seamless cylinder with diameter in nanometer scale and

length from tens of nanometers even to several micrometers if we ignore its two end caps, while a MWNT consists of a series of coaxial SWNTs with layer distance about 3.4\AA [4].

SWNTs have many unique properties. Viewed from the chirality, some of them are chiral but others are achiral. Viewed from the electronic properties, some of them are metallic but others are semiconductive. Moreover, their electronic properties depend sensitively on their chirality [5–8]. The conductivity of metallic SWNT does not satisfy Ohm’s law because the electron transport in it is ballistic [9–11]. Otherwise, theoretical [12–15] and experimental [16] studies have suggested that SWNTs also possess many novel mechanical properties, in particular high stiffness and axial strength, which are insensitive to the tube diameters and chirality. MWNTs have the similar mechanical properties to SWNTs [17–19].

In purely theoretical point of view, we should consider the following two facts:

(i) As quasi-one-dimensional structures with periodic boundary conditions, SWNTs might show anisotropic physical properties which may depend on the tube diameters and chirality. Generally speaking, the physical properties of crystals can be represented by tensors [20]. For example, the electronic conductivity can be expressed by second-rank tensor and the elastic constants can be described as fourth-rank tensor. These tensors can be derived from the structures and symmetries of SWNTs. Therefore fully discussing structures and symmetries of SWNTs is one of the topic in this chapter.

(ii) The SWNT is a single layer of carbon atoms. What is the thickness of the layer? It is a widely controversial question. Some researchers take 3.4\AA , the layer distance of bulk graphite, as the thickness of SWNT [15, 16]. Others define an effective thickness (about 0.7\AA) by admitting the validity of elastic shell theory in nanometer scale [12, 13]. The present authors have proved that the elastic shell theory can indeed be applied to SWNTs [21] which supports the latter standpoint. Because the two standpoints have little effect on the mechanical results in many cases, the controversy is still being discussed [22–28]. Therefore it is necessary to point out when the two standpoints will give different results.

In the applied point of view, the present authors have predicted a molecular motor constructed from a DWNT driven by temperature variation [29] which induces to molecular dynamics simulations by Dendzik *et al.* [30]. Using molecular dynamics simulations, Kang *et al.* recently predicted a carbon-nanotube motor driven by fluidic gas [31]. In this chapter, a conceptual motor of DWNT driven by alternating voltage will be proposed based on previous work [29].

STRUCTURES, SYMMETRIES AND THEIR INDUCING PHYSICAL PROPERTIES OF SWNTS

To describe the SWNT, some characteristic vectors require introducing. As shown in Fig.1, the chiral vector \mathbf{C}_h , which defines the relative location of two sites, is specified by a pair of integers (n, m) which is called the index of the SWNT and relates \mathbf{C}_h to two unit vectors \mathbf{a}_1 and \mathbf{a}_2 of graphite ($\mathbf{C}_h = n\mathbf{a}_1 + m\mathbf{a}_2$). The chiral angle θ_0 defines the angle between \mathbf{a}_1 and \mathbf{C}_h . For (n, m) nanotube, $\theta_0 = \arccos \left[\frac{2n+m}{2\sqrt{n^2+m^2+nm}} \right]$. The translational vector \mathbf{T} corresponds to the first lattice point of 2D graphitic sheet through which the line normal to the chiral vector \mathbf{C}_h passes. The unit cell of the SWNT is the rectangle defined by vectors \mathbf{C}_h and \mathbf{T} , while vectors \mathbf{a}_1 and \mathbf{a}_2 define the area of the unit cell of 2D graphite. The number N of hexagons per unit cell of SWNT is obtained as a function of n and m as $N = 2(n^2 + m^2 + nm)/d_R$ which is larger than 8 for SWNTs in practice, where d_R is the greatest common divisor of $(2m + n)$ and $(2n + m)$. There are $2N$ carbon atoms in each unit cell of SWNT because every hexagon contains two atoms. To denote the $2N$ atoms, we use a symmetry vector \mathbf{R} to generate coordinates of carbon atoms in the nanotube and it is defined as the site vector having the smallest component in the direction of \mathbf{C}_h . From a geometric standpoint, vector \mathbf{R} consists of a rotation around the nanotube axis by an angle $\Psi = 2\pi/N$ combined with a translation τ in the direction of \mathbf{T} ; therefore, \mathbf{R} can be denoted by $\mathbf{R} = (\Psi|\tau)$. Using the symmetry vector \mathbf{R} , we can divide the $2N$ carbon atoms in the unit cell of SWNT into two classes [32]: one includes N atoms whose site vectors satisfy

$$\mathbf{A}_l = l\mathbf{R} - [l\mathbf{R} \cdot \mathbf{T}/\mathbf{T}^2]\mathbf{T} \quad (l = 0, 1, 2, \dots, N-1), \quad (1)$$

another includes the remainder N atoms whose site vectors satisfy

$$\begin{aligned} \mathbf{B}_l = l\mathbf{R} + \mathbf{B}_0 - [(l\mathbf{R} + \mathbf{B}_0) \cdot \mathbf{T}/\mathbf{T}^2]\mathbf{T} \\ - [(l\mathbf{R} + \mathbf{B}_0) \cdot \mathbf{C}_h/\mathbf{C}_h^2]\mathbf{C}_h \quad (l = 0, 1, \dots, N-1), \end{aligned} \quad (2)$$

where $\mathbf{B}_0 \equiv (\Psi_0|\tau_0) = \left(\frac{2\pi r_0 \cos(\theta_0 - \frac{\pi}{6})}{|\mathbf{C}_h|} \middle| r_0 \cos(\theta_0 - \frac{\pi}{6}) \right)$ represents one of the nearest neighbor atoms to \mathbf{A}_0 and r_0 is the carbon-carbon bond length.

If we introduce cylindrical coordinate system (r, θ, z) whose z -axis is the tube axis parallel to vector \mathbf{T} . Its $r\theta$ -plane is perpendicular to z -axis and contains atom A_0 in the nanotube. r the distance from some point to z -axis, and θ the angle rotating around z -axis from an axis which is vertical to z -axis and passes through atom A_0 in the tube to the point. In this coordinate system, we can express Eqs.(1) and (2) as [33]:

$$\mathbf{A}_l = \{ \rho, l\Psi, l\tau - [l\tau/T]T \} \quad (l = 0, 1, 2, \dots, N-1), \quad (3)$$

and

$$\begin{aligned} \mathbf{B}_l = \left\{ \rho, l\Psi + \Psi_0 - 2\pi \left[\frac{l\Psi + \Psi_0}{2\pi} \right], l\tau + \tau_0 - \left[\frac{l\tau + \tau_0}{T} \right] T \right\} \\ (l = 0, 1, 2, \dots, N-1), \end{aligned} \quad (4)$$

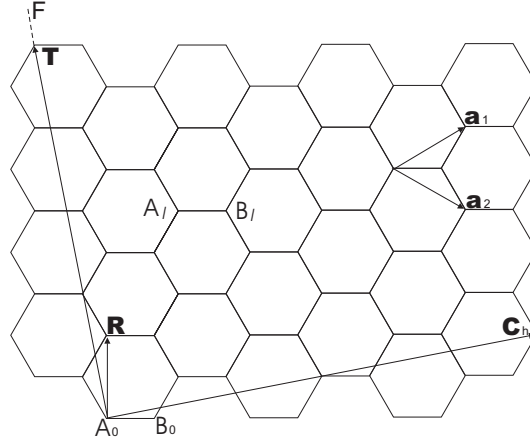


Figure 1: The unrolled honeycomb lattice of a SWNT. By rolling up the sheet along the chiral vector \mathbf{C}_h , that is, such that the point A_0 coincides with the point corresponding to vector \mathbf{C}_h , a nanotube is formed. The vectors \mathbf{a}_1 and \mathbf{a}_2 are the real space unit vectors of the hexagonal lattice. The translational vector \mathbf{T} is perpendicular to \mathbf{C}_h and runs in the direction of the tube axis. The vector \mathbf{R} is the symmetry vector. A_0, B_0 and $A_l, B_l (l = 1, 2, \dots, N)$ are used to denote the sites of carbon atoms.

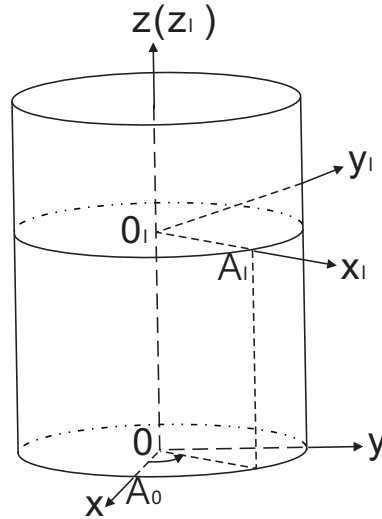


Figure 2: The coordinates of SWNT.

where $\rho = \frac{|C_B|}{2\pi}$. In Eqs.(1)-(4), the symbol $[\dots]$ denotes the largest integer smaller than \dots , e.g., $[7.3] = 7$.

In the following contents of this section, we will derive the general forms of the second, third, and fourth rank tensors by fully considering the symmetries of SWNTs. As shown in Fig.2, xyz is the initial coordinate system whose z -axis is the tube axis and x -axis passes through atom A_0 . If we use \mathbf{R} to act l times on the initial system, we can get the coordinate system $O_l x_l y_l z_l$. Obviously, the transformation from the bases $\hat{x}, \hat{y}, \hat{z}$ of the initial system to the new bases $\hat{x}_l, \hat{y}_l, \hat{z}_l$ can be expressed as,

$$\begin{pmatrix} \hat{x}_l \\ \hat{y}_l \\ \hat{z}_l \end{pmatrix} = (a_{ij}) \begin{pmatrix} \hat{x} \\ \hat{y} \\ \hat{z} \end{pmatrix}, \quad (5)$$

where (a_{ij}) is the matrix with elements $a_{11} = a_{22} = \cos l\psi$, $a_{12} = \sin l\psi$, $a_{21} = -\sin l\psi$, $a_{33} = 1$, $a_{13} = a_{31} = a_{23} = a_{32} = 0$.

Above all, let us consider the second-rank tensor \mathbf{S} . s_{ij} and $s_{ij}^{(l)}$ ($i, j = 1, 2, 3; l = 1, 2, \dots, N$) denote its components in the coordinate system $Oxyz$ and $O_l x_l y_l z_l$. The transformation law of the components is $s_{ij}^{(l)} = a_{im} a_{jk} s_{mk}$ [20], where the Einstein summation convention is used. But the symmetry of SWNTs requires $s_{ij}^{(l)} = s_{ij}$. From this condition and the transformation law we derive out $s_{11} = s_{22}$, $s_{12} = -s_{21}$, $s_{13} = s_{31} = 0$, $s_{23} = s_{32} = 0$. Especially, there are only 2 different nonzero parameters in symmetric 2nd-rank tensors which represent the electronic conductivity or static polarizabilities: $s_{11} = s_{22} \neq 0$, $s_{33} \neq 0$.

Next, let us deal with the third-rank tensor \mathbf{D} whose components are denoted by d_{ijk} and $d_{ijk}^{(l)}$ ($i, j, k = 1, 2, 3$) in the coordinate system $Oxyz$ and $O_l x_l y_l z_l$, respectively. From the transformation law of the components $d_{ijk}^{(l)} = a_{iq} a_{ju} a_{kv} d_{quv}$ [20] and the symmetry of SWNTs, we can obtain the non-vanishing components of \mathbf{D} : $d_{113} = d_{223}$, $d_{123} = -d_{213}$, $d_{131} = d_{232}$, $d_{132} = -d_{231}$, $d_{311} = d_{322}$, $d_{312} = -d_{321}$, d_{333} . If some physical property requires $d_{ijk} = d_{ikj}$ (e.g. the second order polarization effect), then there are only 4 different nonzero parameters in its components: $d_{123} = -d_{213} = d_{132} = -d_{231} \equiv d_1/2$, $d_{113} = d_{223} = d_{131} = d_{232} \equiv d_2/2$, $d_{311} = d_{322} \equiv d_3$, $d_{333} \equiv d_4$. Thus the relation $P_i^{NL} = d_{ijk} E_j E_k$ between the nonlinear polarization and field can be expressed in matrix form,

$$\begin{cases} P_x^{NL} = d_1 E_y E_z + d_2 E_x E_z \\ P_y^{NL} = d_2 E_y E_z - d_1 E_x E_z \\ P_z^{NL} = d_3 (E_x^2 + E_y^2) + d_4 E_z^2 \end{cases}. \quad (6)$$

Similarly, we can obtain the nonzero components of the fourth-rank tensor \mathbf{C} from the transformation law $c_{ijklm}^{(l)} = a_{iq} a_{ju} a_{kv} a_{mw} c_{quvw}$ ($i, j, k, m = 1, 2, 3$) [20] and the symmetry of SWNTs: $c_{1111} = c_{2222}$, $c_{1112} = -c_{2221}$, $c_{1121} = -c_{2212}$, $c_{1122} = c_{2211}$, $c_{1133} = c_{2233}$, $c_{1211} = -c_{2122}$, $c_{1212} = c_{2121}$, $c_{1221} = c_{2112} = c_{2222} - c_{2121} - c_{2211}$, $c_{2111} = -c_{1222} = c_{2122} + c_{2212} + c_{2221}$, $c_{1233} = -c_{2133}$, $c_{1313} = c_{2323}$, $c_{1323} = -c_{2313}$, $c_{1331} = c_{2332}$, $c_{1332} = -c_{2331}$, $c_{3113} = c_{3223}$, $c_{3123} = -c_{3213}$,

$c_{3131} = c_{3232}$, $c_{3132} = -c_{3321}$, $c_{3311} = c_{3322}$, $c_{3312} = -c_{3321}$, c_{3333} . If we consider the elastic property, the elastic constants can be expressed by the fourth-rank tensor whose components satisfy $c_{ijklm} = c_{ijmkl} = c_{jiklm} = c_{kmlij}$ [20]. Thus there are only 5 different non-vanishing parameters (c_1, c_2, c_3, c_4, c_5) in its components and $c_{1111} = c_{2222} \equiv c_1$, $c_{1133} = c_{3311} = c_{2233} = c_{3322} \equiv c_2$, $c_{3333} = c_3$, $c_{1313} = c_{2323} = c_{1331} = c_{2332} = c_{3113} = c_{3223} = c_{3131} = c_{3232} \equiv c_4$, $c_{1122} = c_{2211} \equiv c_5$, $c_{1212} = c_{2121} = c_{1221} = c_{2112} = (c_1 - c_5)/2$. The stress-strain relation $\boldsymbol{\sigma} = \mathbf{C}\boldsymbol{\varepsilon}$ can be expressed by the matrix notations,

$$\begin{pmatrix} \sigma_{xx} \\ \sigma_{yy} \\ \sigma_{zz} \\ \sigma_{yz} \\ \sigma_{xz} \\ \sigma_{xy} \end{pmatrix} = \begin{pmatrix} c_1 & c_5 & c_2 & & & \\ & c_5 & c_1 & c_2 & & \\ & c_2 & c_2 & c_3 & & \\ & & & & c_4 & \\ & & & & & c_4 \\ & & & & & & \frac{(c_1 - c_5)}{2} \end{pmatrix} \begin{pmatrix} \varepsilon_{xx} \\ \varepsilon_{yy} \\ \varepsilon_{zz} \\ \gamma_{yz} \\ \gamma_{xz} \\ \gamma_{xy} \end{pmatrix}, \quad (7)$$

where $\gamma_{xy} = 2\varepsilon_{xy}$, $\gamma_{xz} = 2\varepsilon_{xz}$, $\gamma_{yz} = 2\varepsilon_{yz}$ [34]. The axial Young's modulus Y_z defined as the stress/strain ratio when the tube is axially strained and Poisson ratio ν_z defined as the ratio of the reduction in radial dimension to the axial elongation can be expressed as $Y_z = c_3 - 2c_2^2/(c_1 + c_5)$ and $\nu_z = c_2/(c_1 + c_5)$, respectively.

Obviously, the numbers of different parameters in the expressions \mathbf{S} , \mathbf{D} , \mathbf{C} of SWNTs are more than that in isotropic materials (see also Table 1) if the different parameters are independent, which implies that SWNTs might possess anisotropic physical properties. All parameters are functions of n , m , which reveals the physical properties depend on the chirality and diameters of SWNTs to some extent.

Table 1: The non-zero parameter numbers of different rank physical property tensors for isotropic materials and single-walled carbon nanotubes.

Tensors	\mathbf{S} (2nd-rank)	\mathbf{D} (3rd-rank)	\mathbf{C} (4th-rank)
Isotropic materials	1	0	2
carbon nanotubes	2	4	5

As examples, we will give the forms of second and fourth-rank order tensors—the static polarizabilities and elastic constants of SWNTs, respectively.

It is well known that the relation between the polarization \mathbf{P} and external electric field \mathbf{E} is $\mathbf{P} = \boldsymbol{\alpha}\mathbf{E}$ [35], where $\boldsymbol{\alpha}$ is the static polarizability, a second-rank tensor. From above discussions, we known $\boldsymbol{\alpha}$ can be expressed as matrix form,

$$\boldsymbol{\alpha} = \begin{pmatrix} \alpha_{xx} & & \\ & \alpha_{yy} & \\ & & \alpha_{zz} \end{pmatrix}, \quad (8)$$

with $\alpha_{xx} = \alpha_{yy}$. Benedict *et al.* [36] have studied the polarizabilities and their results are shown in Table 2, where we have changed their values to polarizabilities per atom. From Table 2 we find that the polarizabilities of SWNTs are sensitive to the tube indexes (n, m) , particularly, the value of α_{zz} is extremely large when $n - m$ is a multiple of three, which corresponds metallic tubes.

Table 2: Static polarizabilities per atom of various tube indexes and radii [36]. When $n - m$ is multiple of three, α_{zz} is extremely large and is not given.

(n, m)	$\rho(\text{\AA})$	$\alpha_{zz}(\text{\AA}^3/\text{atom})$	$\alpha_{xx}(\text{\AA}^3/\text{atom})$
(9,0)	3.57		1.05
(10,0)	3.94	18.62	1.10
(11,0)	4.33	17.04	1.20
(12,0)	4.73		1.23
(13,0)	5.12	23.98	1.29
(4,4)	2.73		0.92
(5,5)	3.41		1.02
(6,6)	4.10		1.13
(4,2)	2.09	9.87	0.84
(5,2)	2.46		0.89

Otherwise, we calculate the elastic constants of SWNTs through the tight binding method [13] with considering the curvature and bond-length change effects. The results are listed in Table 3 which suggests that the elastic properties of SWNTs slightly depend on the tube indexes (n, m) . We also give the corresponding axial Young's moduli and Poisson ratios of single-walled carbon nanotubes with different indexes. Moreover, we find $(c_1 + c_5) - c_4 \approx c_2$, $c_3 \approx 2(c_1 + c_5)$ and $(c_1 + c_5) \approx 4c_2$, i.e., there might be only two independent parameters in the elastic constants, which implies that the mechanical anisotropy of SWNTs is so weakly that we can regard them as approximately isotropic materials (Remark: the isotropic materials have two independent elastic constants, see also Table 1).

It is necessary to discuss the meanings of strains and stresses in nanometer scale. Strains are geometric quantities so that their definitions in macroscopic theory of elasticity still hold for SWNTs. But we must redefine stresses because they are not well-defined quantities for SWNTs. Given strains, we can calculate the energy variation of the SWNTs due to the strains through quantum mechanics in principle. The stresses are defined as the partial derivatives of energy variation with respect to the strains. In fact, stresses are not necessary concepts. We can directly determine the elastic constants by strains and the corresponding energy variation.

Otherwise, we do not separate c_1 and c_5 in Table 3. Up to now, we do not know how to separate them. A possibility is that we need not do that when we discuss the mechanical properties of SWNTs.

Table 3: The elastic constants (unit: eV/atom) and corresponding axial Young's moduli (unit: eV/atom), Poisson ratios of single-walled carbon nanotubes.

(n,m)	$c_1 + c_5$	c_2	c_3	c_4	Y_z	ν_z
(6,0)	29.04	7.03	56.97	22.72	53.56	0.24
(8,0)	29.34	7.05	57.68	23.43	54.29	0.24
(10,0)	29.50	7.07	57.92	23.79	54.53	0.24
(50,0)	29.51	7.08	58.97	24.36	55.57	0.24
(6,6)	29.99	7.08	56.97	24.09	53.63	0.24
(8,8)	29.76	7.08	57.92	24.22	54.55	0.24
(10,10)	29.66	7.08	58.33	24.28	54.96	0.24
(50,50)	29.51	7.08	59.00	24.38	55.60	0.24
(6,4)	30.21	7.07	56.15	23.13	52.83	0.23
(7,3)	30.00	7.07	56.60	22.53	53.27	0.24
(8,2)	29.64	7.07	57.44	22.62	54.07	0.24

MECHANICAL PROPERTIES OF CNTS

In this section, we will continue to discuss the mechanical properties of CNTs in detail.

We start from the concise formula proposed by Lenosky *et al.* in 1992 to describe the deformation energy of a single layer of curved graphite [37]

$$\begin{aligned}
 E^g = & (\epsilon_0/2) \sum_{(ij)} (r_{ij} - r_0)^2 + \epsilon_1 \sum_i \left(\sum_{(j)} \mathbf{u}_{ij} \right)^2 \\
 & + \epsilon_2 \sum_{(ij)} (1 - \mathbf{n}_i \cdot \mathbf{n}_j) + \epsilon_3 \sum_{(ij)} (\mathbf{n}_i \cdot \mathbf{u}_{ij}) (\mathbf{n}_j \cdot \mathbf{u}_{ji}). \quad (9)
 \end{aligned}$$

The first two terms are the contributions of bond length and bond angle changes to the energy. The last two terms are the contributions of the π -electron resonance. In the first term, $r_0 = 1.42 \text{ \AA}$ is the initial bond length of planar graphite, and r_{ij} is the bond length between atoms i and j after the deformations. In the remaining terms, \mathbf{u}_{ij} is a unit vector pointing from atom i to its neighbor j , and \mathbf{n}_i is the unit vector normal to the plane determined by the three neighbors of atom i . The summation $\sum_{(j)}$ is taken over the three nearest neighbor j atoms to i atom, and $\sum_{(ij)}$ taken over all the nearest neighbor atoms. The parameters $(\epsilon_1, \epsilon_2, \epsilon_3) = (0.96, 1.29, 0.05)\text{eV}$ were determined by Lenosky *et al.* [37] through local density approximation. The value of ϵ_0 was not given by Lenosky *et al.*, but given by Zhou *et al.* [38] $\epsilon_0 = 57\text{eV}/\text{\AA}^2$ from the force-constant method.

In 1997, Ou-Yang *et al.* [39] reduced Eq.(9) into a continuum limit form without taking the bond length change into account and obtained the curvature

elastic energy of a SWNT

$$E^{(s)} = \int \left[\frac{1}{2} k_c (2H)^2 + \bar{k}_1 K \right] dA, \quad (10)$$

where the bending elastic constant

$$k_c = (18\epsilon_1 + 24\epsilon_2 + 9\epsilon_3)r_0^2/(32\Omega) = 1.17\text{eV} \quad (11)$$

with $\Omega = 2.62 \text{ \AA}^2$ being the occupied area per atom, and

$$\bar{k}_1/k_c = -(8\epsilon_2 + 3\epsilon_3)/(6\epsilon_1 + 8\epsilon_2 + 3\epsilon_3) = -0.645. \quad (12)$$

In Eq.(10), H , K , and dA are mean curvature, Gaussian curvature, and area element of the SWNTs surface, respectively.

In 2002, we obtained the total free energy [21] of a strained SWNT with in-plane strain $\varepsilon_i = \begin{pmatrix} \varepsilon_x & \varepsilon_{xy} \\ \varepsilon_{xy} & \varepsilon_y \end{pmatrix}$ at the i -atom site, where ε_x , ε_y , and ε_{xy} are the axial, circumferential, and shear strains, respectively. The total free energy contains two parts: one is the curvature energy expressed as Eq.(10); another is the deformation energy [21]

$$E_d = \int \left[\frac{1}{2} k_d (2J)^2 + \bar{k}_2 Q \right] dA, \quad (13)$$

where $2J = \varepsilon_x + \varepsilon_y$ and $Q = \varepsilon_x \varepsilon_y - \varepsilon_{xy}^2$, are respectively named ‘‘mean’’ and ‘‘Gaussian’’ strains, and

$$k_d = 9(\epsilon_0 r_0^2 + \epsilon_1)/(16\Omega) = 24.88\text{eV}/\text{\AA}^2, \quad (14)$$

$$\bar{k}_2 = -3(\epsilon_0 r_0^2 + 3\epsilon_1)/(8\Omega) = -0.678k_d. \quad (15)$$

The value of \bar{k}_2/k_d is so excellently close to the value of \bar{k}_1/k_c shown in Eq.(12) that we can regard that they are, in fact, equal to each other. We assume both \bar{k}_2/k_d and \bar{k}_1/k_c are equal to their average value,

$$\bar{k}_1/k_c = \bar{k}_2/k_d = -0.66. \quad (16)$$

This is the key relation that allows to describe the deformations of SWNT with classic elastic theory. Thus, the deformation energy of a SWNT, the sum of Eqs.(10) and (13)

$$E_d^{(s)} = \int \left[\frac{1}{2} k_c (2H)^2 + \bar{k}_1 K \right] dA + \int \left[\frac{1}{2} k_d (2J)^2 + \bar{k}_2 Q \right] dA \quad (17)$$

can be expressed as the form of the classic shell theory [34]:

$$\begin{aligned} E_c &= \frac{1}{2} \int D [(2H)^2 - 2(1-\nu)K] dA \\ &+ \frac{1}{2} \int \frac{C}{1-\nu^2} [(2J)^2 - 2(1-\nu)Q] dA, \end{aligned} \quad (18)$$

where $D = (1/12)Yh^3/(1 - \nu^2)$ and $C = Yh$ are bending rigidity and in-plane stiffness of shell. ν is the Poisson ratio and h is the thickness of shell. Comparing Eq.(17) with Eq.(18), we have

$$\begin{cases} (1/12)Yh^3/(1 - \nu^2) = k_c \\ Yh/(1 - \nu^2) = k_d \\ 1 - \nu = -\bar{k}_1/k_c = -\bar{k}_2/k_d \end{cases}. \quad (19)$$

From above equations we obtain the Poisson ratio, effective wall thickness, and Young's modulus of SWNTs are $\nu = 0.34$, $h = 0.75\text{\AA}$ and, $Y = 4.70\text{TPa}$, respectively. Our numerical results are close to those given by Yakobson *et al.* [12].

Through above discussion, we can declare that: (i) Eqs.(16), (17) and (18) imply that elastic shell theory in macroscopic scale can be applied to the SWNT in mesoscopic scale provided that its radius are not too small. (ii) SWNT can be regard as being made from isotropic materials with $Y = 4.70\text{TPa}$ and $\nu = 0.34$. Its effective thickness can be well-defined as $h = 0.75\text{\AA}$.

We now turn to discuss the axial Young's modulus of MWNT. A MWNT can be thought of as a series of coaxial SWNTs with layer distance $d = 3.4\text{\AA}$.

Due to the deformation energy of SWNT, we can write the deformation energy of MWNT as [21]

$$\begin{aligned} E^{(m)} &= \sum_{l=1}^N \int \left[\frac{1}{2}k_d(2J)^2 + \bar{k}_2Q \right] dA \\ &+ \sum_{l=1}^N \pi k_c L / \rho_l + \sum_{l=1}^{N-1} (\Delta E_{coh}/d) \pi L (\rho_{l+1}^2 - \rho_l^2), \end{aligned} \quad (20)$$

where ρ_l is the radius of the l -th layer from inner one, N is the layer number of MWNT, and $\Delta E_{coh} = -2.04\text{eV/nm}^2$ [40] being the interlayer cohesive energy per area of planar graphite. L is the length of MWNT. The second term in Eq.(20) expresses the summation of curvature energies on all layers given in Eq.(10), and the third term represents the total interlayer cohesive energy which actually arises from the relatively weaker Van der Waals' interactions. On this account, we can reasonably believe that the axial strain ε_x and circumferential strain ε_y still satisfy $\varepsilon_y = -\nu\varepsilon_x$ for every layer of SWNT in the MWNT when uniform stresses apply along axial direction. Thus Eq.(20) becomes

$$E^{(m)} = \frac{k_d}{2}(1 - \nu^2)\varepsilon_x^2 \sum_{l=1}^N 2\pi\rho_l L + \sum_{l=1}^N \pi k_c L / \rho_l + \sum_{l=1}^{N-1} \Delta E_{coh} \pi L (\rho_{l+1} + \rho_l). \quad (21)$$

The axial Young's modulus of the MWNT Y_m is defined as

$$Y_m(N) = \frac{1}{V} \frac{\partial^2 E^{(m)}}{\partial \varepsilon_x^2}, \quad (22)$$

where $V = \pi L[(\rho_N + h/2)^2 - (\rho_1 - h/2)^2]$ is the volume of MWNT. If considering $\sum_{l=1}^N 2\pi\rho_l L = (\rho_1 + \rho_N)N\pi L$, from Eqs.(21) and (22) we have [21]

$$Y_m(N) = \frac{N}{N-1+h/d} \frac{h}{d} Y, \quad (23)$$

where Y and h are the Young's modulus and effective wall thickness of SWNTs. Obviously, $Y_m = Y = 4.70\text{TPa}$ if $N=1$, which corresponds to the result of SWNTs, and $Y_m = Yh/d = 1.04\text{TPa}$ if $N \gg 1$, which is just the Young's modulus of bulk graphite. The layer number dependence of MWNT's Young's modulus can be used to discuss mechanical properties of nanotube/polymer composites [41–43].

Now let us discuss the mechanical stabilities of SWNTs and MWNTs. In above discussion, we have prove that elastic shell theory can be applied to SWNTs. Thus we can directly use the classical results in elastic shell theory [44, 45].

The critical pressure for SWNT by axial stress on both free ends is

$$p_{csa} = \frac{1}{\sqrt{3(1-\nu^2)}} \frac{Yh}{\rho}. \quad (24)$$

The critical pressure for SWNT (with two free ends) by radial stress is

$$p_{csr} = \frac{Yh^3}{4(1-\nu^2)\rho^3}. \quad (25)$$

The critical moment for SWMT by uniform bending moment is

$$M_{cs} = \frac{2\sqrt{2}\pi Y \rho h^2}{9\sqrt{1-\nu^2}}. \quad (26)$$

The critical torsion for SWMT by uniform torsion is

$$T_{cs} = \frac{\sqrt{2}\pi Y \sqrt{\rho h^5}}{3(1-\nu^2)^{3/4}}. \quad (27)$$

In above four equations, $\nu = 0.34$, $h = 0.75\text{\AA}$, $Y = 4.70\text{TPa}$, and ρ is the radius of SWNT.

The stability of MWNT is determined by its weakest layer of SWNT. Thus we have the critical pressure for MWNT by axial stress on both free ends

$$p_{cma} = \frac{1}{\sqrt{3(1-\nu^2)}} \frac{Yh}{\rho_o} \quad (28)$$

and the critical pressure for MWNT (with two free ends) by radial stress

$$p_{cmr} = \frac{Yh^3}{4(1-\nu^2)\rho_o^3}, \quad (29)$$

where $\nu = 0.34$, $h = 0.75\text{\AA}$, $Y = 4.70\text{TPa}$, and ρ_o is the outmost radius of MWNT.

Eqs.(24)–(29) are valid provided that the elastic shell theory can be applied to SWNTs. Adopting the *ad hoc* convention $h = 3.4\text{\AA}$ —the layer distance of bulk graphite as the thickness of SWNTs will give different values of these equations. Thus the crucial experiments to test above relations will judge whether we should take the *ad hoc* convention or effective thickness of SWNTs.

MOTORS OF DWNTS

With the development of nanotechnology, especially the discovery of carbon nanotubes, people are putting their dream of manufacturing nanodevices [46,47] into practice. In this section, we will discuss the potential application of CNTs. First, we specifically introduce a molecular motor constructed from a DWNT driven by temperature variation due to the different chirality of DWNT proposed in Ref. [29]. As shown in Fig.3, inner tube's index is (8, 4) with a length long enough to be regarded as infinite while outer tube is a (14, 8) tube with just a single unit cell [48]. Obviously, they are both chiral nanotubes and their layer distance is about 3.4 Å. If we prohibit the motion of outer tube in the direction of nanotube axis, it will be proved that, in a thermal bath, outer tube exhibits a directional rotation when the temperature of the bath varies with time. Thus it could serve as a thermal ratchet.

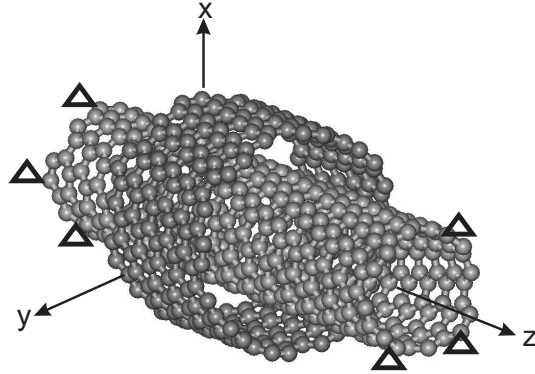


Figure 3: A double-walled carbon nanotube with inner tube's index being (8, 4) and outer tube's index being (14, 8). z -axis is the tube axis parallel to vector \mathbf{T} . x -axis is perpendicular to z passes through one of carbon atoms in inner tube and y -axis perpendicular to the xz -plane. The triangles represent the fixed devices of outer tube. There is no obviously relative motion along radial direction between inner and outer tubes at low temperature. If we forbid the motion of outer tube in the direction of z -axis, only the rotation of outer tube around inner tube is permitted.

To see this, we first select an orthogonal coordinate system shown in Fig.3 whose z -axis is the tube axis and x -axis passes through one of carbon atoms in the inner tube. We fix the inner tube and forbid the z -directional motion of the outer tube. The rotation angle of outer tube around the inner one is denoted by θ .

We take the interaction between atoms in outer and inner tube as the Lennard-Jones potential $u(r_{ij}) = 4\epsilon[(\sigma/r_{ij})^{12} - (\sigma/r_{ij})^6]$, where r_{ij} is the distance between atom i in inner tube and atom j in outer tube, $\epsilon = 28$ K, and $\sigma = 3.4\text{\AA}$ [49]. We calculate the potential $V(\theta)$ when outer tube rotates around inner tube with angle θ and plot it in Fig.4.

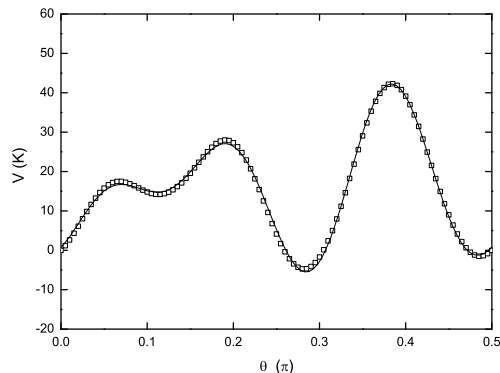


Figure 4: The potentials $V(\theta)$ between outer and inner tubes when outer tube rotates around inner tube. θ is the rotating angle. Here we have set $V(0) = 0$. The squares are the numerical results which can be well fitted by $V(\theta) = 15.7 - 0.6 \cos 4\theta - 2.2 \sin 4\theta - 12.7 \cos 8\theta - 6 \sin 8\theta - 1.7 \cos 12\theta + 10.8 \sin 12\theta$ (solid curve).

If putting our system in a thermal bath full of He gas whose temperature varies with time, We can show that outer tube will exhibit a directional rotation. Let us consider the overdamped case when the Langevin equation for outer tube is expressed

$$\eta \dot{\theta} = -V'(\theta) + \xi(t), \quad (30)$$

where η is the rotating viscosity coefficient, and dot and prime indicate, respectively, differentiations with respect to time t and angle θ . $\xi(t)$ is thermal noise which satisfies $\langle \xi(t) \rangle = 0$ and the fluctuation-dissipation relation $\langle \xi(t)\xi(s) \rangle = 2\eta T(t)\delta(t-s)$, where $T(t)$ is temperature and the Boltzmann factor is set to 1. The Fokker-Planck equation corresponding to Eq.(30) is [50]:

$$\frac{\partial P(\theta, t)}{\partial t} = \frac{\partial}{\partial \theta} \left[\frac{V'(\theta)P(\theta, t)}{\eta} \right] + \frac{T(t)}{\eta} \frac{\partial^2 P(\theta, t)}{\partial \theta^2}, \quad (31)$$

where $P(\theta, t)$ represents the probability of finding the outer tube at angle θ and time t which satisfies $P(\theta + \pi/2, t) = P(\theta, t)$. If the period of temperature

variation is \mathcal{T} , we arrive at the average angular velocity in the long-time limit [50]

$$\langle \dot{\theta} \rangle = \lim_{t \rightarrow \infty} \frac{1}{\mathcal{T}} \int_t^{t+\mathcal{T}} dt \int_0^{\pi/2} d\theta \left[-\frac{V'(\theta)P(\theta, t)}{\eta} \right]. \quad (32)$$

Here we take the periodical varying temperature $T(t) = \bar{T}[1 + A \sin(2\pi t/\mathcal{T})]$ with $\bar{T} = 50$ K and $|A| \ll 1$. Changing variables $D = \eta/\bar{T}$, $t = D\tau$, $U(\theta) = V(\theta)/\bar{T}$, $\mathcal{T} = D\mathcal{J}$ and $\tilde{P}(\theta, \tau) = P(\theta, D\tau)$, We arrive at the dimensionless equations of Eqs.(31) and (32)

$$\frac{\partial \tilde{P}}{\partial \tau} = \frac{\partial}{\partial \theta} [U'(\theta)\tilde{P}] + (1 + A \sin \frac{2\pi\tau}{\mathcal{J}}) \frac{\partial^2 \tilde{P}}{\partial \theta^2}, \quad (33)$$

$$\langle \frac{d\theta}{d\tau} \rangle = \lim_{\tau \rightarrow \infty} \frac{1}{\mathcal{J}} \int_{\tau}^{\tau+\mathcal{J}} d\tau \int_0^{\pi/2} d\theta \left[-U'(\theta)\tilde{P} \right]. \quad (34)$$

We numerically solve Eq.(33) and calculate Eq.(34) with $A = 0.01$ and different \mathcal{J} . The curve in Fig.5 shows the relation between the average dimensionless angular velocity $\langle \frac{d\theta}{d\tau} \rangle$ and the dimensionless period \mathcal{J} of temperature variation. We find that $\langle \frac{d\theta}{d\tau} \rangle \simeq 0$ for very small and large \mathcal{J} , and $\langle \frac{d\theta}{d\tau} \rangle \neq 0$ for the middle values of \mathcal{J} , which implies that outer tube has an evident directional rotation in this period range.

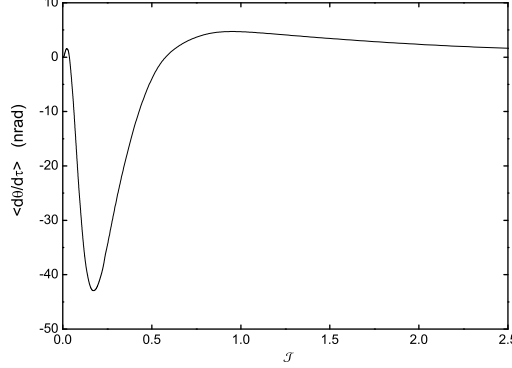


Figure 5: The average dimensionless angular velocity $\langle d\theta/d\tau \rangle$ of outer tube rotating around inner tube in thermal bath whose temperature changes with dimensionless period \mathcal{J} . The minus sign means rotation around z -axis is the left-handed, and vice versa.

In above discussion, we have conceptually constructed a temperature ratchet—a kind of molecular motor driven by temperature variations which satisfies two necessary conditions required by the second law of thermodynamics [51]: One is breaking spatial inversion symmetry (through different chirality of two SWNTs in DWNT); Another is breaking of thermal equilibrium (through temperature

variations). But, in fact, this motor is not convenient because it is hard to control temperature variations. Our dream is to construct an electric motor driven by alternating voltage discussed as below.

Although no one believes SWNTs are piezoelectric materials, an exceptionally large axial deformation in SWNTs induced by applied electrostatic field along tube axis is demonstrated using Hartree-Fock and density functional calculations by Guo *et al.* [52]. Additionally, their calculations reveal that the bond-elongation of SWNTs is linearly dependent on the axial field when the field is not strong enough. These results shed a light on our dream of making the electric motor. Now, we will qualitatively construct it. Put the device shown in Fig.3 between two electrodes and apply alternating voltage $U_A(t) = U_0 \sin(\omega t)$ on the electrodes, where U_0 and ω are constants. We expect that the field due to alternating voltage also induces bond-elongation of the DWNT. Thus the layer distance will change, which will change the interaction between layers. At least for small U_0 , the lowest order Taylor Series of interaction between layers might be written as $\tilde{V}(\theta, t) \approx V(\theta) + \delta(\theta)|\sin \omega t|$ with $\delta(\theta)$ being a small quantity. If putting our system in a thermal bath full of He gas with constant temperature T , we have the Langevin equation of outer tube in the overdamped case [50]:

$$\eta \dot{\theta} = -[V'(\theta) + \delta'(\theta)|\sin \omega t|] + \xi(t), \quad (35)$$

where $\xi(t)$ is thermal noise which satisfies $\langle \xi(t) \rangle = 0$ and the fluctuation-dissipation relation $\langle \xi(t)\xi(s) \rangle = 2\eta T \delta(t-s)$. Consequently, the thermal equilibrium is broken by the shaking potential $\tilde{V}(\theta, t)$, and we may construct a fluctuating potential ratchet proposed in Ref. [50, 53].

CONCLUSION

In this chapter, we introduce the structures, symmetries and their inducing physical properties of SWNTs in detail. We discuss the mechanics of nanotubes and explain why we must define the effective thickness of SWNTs. We also qualitatively construct an electric motor driven by alternating voltage. We expect some experiments which can put our electric motor into practice in near future.

References

- [1] Kroto, H. *et al.* *Nature* 1985, *318*, 162-163.
- [2] Iijima, S. *Nature* 1991, *354*, 56-58.
- [3] Iijima, S.; Ichihashi, T. *Nature* 1993, *363*, 603-605.
- [4] Saito, R.; Dresselhaus, M. S.; Dresselhaus, G. *Physical Properties of Carbon Nanotubes*; Imperial College Press: London, 1998; pp 35-48.

- [5] Mintmire, J. W.; Dunlap, B. I.; White, C. T. *Phys. Rev. Lett.* 1992, *68*, 631-634.
- [6] Hamada, N.; Sawada, S. I.; Oshiyama, A. *Phys. Rev. Lett.* 1992, *68*, 1579-1581.
- [7] Saito, R.; Fujita, M.; Dresselhaus, G.; Dresselhaus, M. S. *Appl. Phys. Lett.* 1992, *60*, 2204-2206.
- [8] Tans, S. J. *et al. Nature* 1997, *386*, 474-477.
- [9] Kong, J. *et al. Phys. Rev. Lett.* 2001, *87*, 106801.
- [10] Liang, W. J. *et al. Nature* 2001, *411*, 665-669.
- [11] White, C. T.; Todorov, T. N. *Nature* 1998, *393*, 240-242.
- [12] Yakobson, B. I.; Brabec, C. J.; Bernholc, J. *Phys. Rev. Lett.* 1996, *76*, 2511-2514.
- [13] Zhou, X.; Zhou, J. J.; Ou-Yang, Z. C. *Phys. Rev. B* 2000, *62*, 13692-13696.
- [14] Hernández, E. *et al. Phys. Rev. Lett.* 1998, *80*, 4502-4505.
- [15] Lu, J. P. *Phys. Rev. Lett.* 1997, *79*, 1297-1300.
- [16] Krishnan, A. *et al. Phys. Rev. B* 1998, *58*, 14013-14019.
- [17] Yu, M. F. *et al. Science* 2000, *287*, 637-640.
- [18] Treacy, M. M. J.; Ebbesen, T. W.; Gibson, J. M. *Nature* 1996, *381*, 678-680.
- [19] Wong, E. W.; Sheehan, P. E.; Lieber, C. M. *Science* 1997, *277* 1971-1975.
- [20] Nye, J. F. *Physical Properties of Crystals*; Clarendon Press: Oxford, 1985; pp 33-148.
- [21] Tu, Z. C.; Ou-Yang, Z. C. *Phys. Rev. B* 2002, *65*, 233407.
- [22] Rafii-Tabar, H. *Phys. Rep.* 2004, *390*, 235-452.
- [23] Pantano, A.; Parks, D. M.; Boyce, M. C. *J. Mech. Phys. Solids* 2004, *52* 789-821.
- [24] Chandra, N. *et al. Phys. Rev. B* 2004, *69*, 94101.
- [25] Ogata, S. *et al. Phys. Rev. B* 2003, *68*, 165409.
- [26] Pantano, A. *et al. Phys. Rev. Lett.* 2003, *91*, 145504.
- [27] Natsuki, T.; Tantrakarn, K.; Endo, M. *Appl. Phys. A-Mater.* 2004, *79*, 117-124.
- [28] Sun, C. Q. *et al. J Phys Chem B* 2003, *107*, 7544-7546.

- [29] Tu, Z. C.; Ou-Yang Z. C. *J. Phys.: Condens. Matter* 2004, *16*, 1287-1292.
- [30] Dendzik, Z. *et al. Poster at E-MRS Fall Meeting* 2004, Symposium H, Poland.
- [31] Kang, J. W. *et al. J. Korean Phys. Soc.* 2004, *45*, 573-576.
- [32] Tu, Z. C.; Ou-Yang Z. C. *Phys. Rev. B* 2003, *68*, 153403.
- [33] Tu, Z. C.; Ou-Yang Z. C. *J. Phys.: Condens. Matter* 2003, *15*, 6759-6771.
- [34] Landau, L. D.; Lifshiz, E. M. *Elasticity Theory*; Pergamon: Oxford, 1986.
- [35] Landau, L. D.; Lifshiz, E. M. *Electrodynamics of Continuous Media*; Pergamon: Oxford, 1984.
- [36] Benedict, L. X.; Louie, S. G.; Cohen, M. L. *Phys. Rev. B* 1995, *52*, 8541-8549.
- [37] Lenosky, T. *et al. Nature* 1992 *355*, 333-335.
- [38] Zhou, X.; Zhou, J. J.; Ou-Yang, Z. C. *Physica B* 2001, *304*, 86-90.
- [39] Ou-Yang, Z. C.; Su, Z. B.; Wang, C. L. *Phys. Rev. Lett.* 1997, *78*, 4055-4058.
- [40] Girifalco, L. A.; Lad, R. A. *J. Chem. Phys.* 1956, *25*, 693.
- [41] Lau, K. T. *Chem. Phys. Lett.* 2003 *370*, 399-405.
- [42] Lau, K. T.; Shi, S. Q. *Carbon* 2002, *40*, 2965-2968.
- [43] Xiao, T.; Liao, K. *Compos. Part. B-Eng.* 2004, *35* 211-217.
- [44] Wu, J. K.; Su, X. Y. *Stabilities of Elastic Systems*; Science Press: Beijing, 1994.
- [45] Pogorelov, A. V. *Bendings of surfaces and stability of shells*; AMS: Providence, 1989.
- [46] Feynman, R. P. *J. Microelectromechanical Systems* 1992, *1*, 60.
- [47] Drexler, K. E. *Nanosystems: Molecular Machinery, Manufacturing and Computation*; Wiley: New York, 1992.
- [48] If we consider several unit cells, the final qualitative results still hold.
- [49] Hirschfelder, J. O.; Curtiss, C. F.; Bird, R. B. *Molecular Theory of Gases and Liquids*; John Wiley & Sons: New York, 1954.
- [50] Reimann, P. *Phys. Rep.* 2002, *361*, 57-265.
- [51] Feynman, R. P.; Leighton, R. B.; Sands, M. *The Feynman Lectures on Physics*; Addison-Wesley: Reading, 1966; *Vol 1*, Chapter 46.

[52] Guo, W.; Guo, F. *Phys. Rev. Lett.* 2003, *91*, 115501.

[53] Astumian, R. D.; Bier, M. *Phys. Rev. Lett.* 1994, *72*, 1766-1769.